European Heart Journal (2012) **33**, 1942–1953
doi:10.1093/eurheartj/ehr472

CLINICAL RESEARCH
Heart failure/cardiomyopathy

Electrophysiological abnormalities precede overt structural changes in arrhythmogenic right ventricular cardiomyopathy due to mutations in desmoplakin-A combined murine and human study

John Gomes[1], Malcolm Finlay[2], Akbar K. Ahmed[2], Edward J. Ciaccio[3], Angeliki Asimaki[4], Jeffrey E. Saffitz[4], Giovanni Quarta[2], Muriel Nobles[1,5], Petros Syrris[2], Sanjay Chaubey[6], William J. McKenna[2], Andrew Tinker[1,5]*, and Pier D. Lambiase[2]*

[1]Department of Medicine, UCL, London, UK; [2]Institute of Cardiovascular Sciences, UCL, London, UK; [3]Columbia University, NY, USA; [4]Beth Israel Deaconess Medical Centre, Boston, MA, USA; [5]William Harvey Heart Centre, London, UK; and [6]King's College, London, UK

Received 28 July 2011; revised 2 November 2011; accepted 1 December 2011; online publish-ahead-of-print 11 January 2012

Aims Anecdotal observations suggest that sub-clinical electrophysiological manifestations of arrhythmogenic right ventricular cardiomyopathy (ARVC) develop before detectable structural changes ensue on cardiac imaging. To test this hypothesis, we investigated a murine model with conditional cardiac genetic deletion of one desmoplakin allele (DSP ±) and compared the findings to patients with non-diagnostic features of ARVC who carried mutations in desmoplakin.

Methods and results *Murine*: the DSP (±) mice underwent electrophysiological, echocardiographic, and immunohistochemical studies. They had normal echocardiograms but delayed conduction and inducible ventricular tachycardia associated with mislocalization and reduced intercalated disc expression of Cx43. Sodium current density and myocardial histology were normal at 2 months of age. *Human*: ten patients with heterozygous mutations in DSP without overt structural heart disease (DSP+) and 12 controls with supraventricular tachycardia were studied by high-density electrophysiological mapping of the right ventricle. Using a standard S_1–S_2 protocol, restitution curves of local conduction and repolarization parameters were constructed. Significantly greater mean increases in delay were identified particularly in the outflow tract vs. controls ($P < 0.01$) coupled with more uniform wavefront progression. The odds of a segment with a maximal activation–repolarization interval restitution slope >1 was 99% higher (95% CI: 13%; 351%, $P = 0.017$) in DSP+ vs. controls. Immunostaining revealed Cx43 mislocalization and variable Na channel distribution.

Conclusion Desmoplakin disease causes connexin mislocalization in the mouse and man preceding any overt histological abnormalities resulting in significant alterations in conduction–repolarization kinetics prior to morphological changes detectable on conventional cardiac imaging. Haploinsufficiency of desmoplakin is sufficient to cause significant Cx43 mislocalization. Changes in sodium current density and histological abnormalities may contribute to a worsening phenotype or disease but are not necessary to generate an arrhythmogenic substrate. This has important implications for the earlier diagnosis of ARVC and risk stratification.

Keywords Arrhythmia • Conduction • ARVC • Repolarization • Desmosome • Desmoplakin

* Corresponding author. The Heart Hospital, University College Hospital and Institute of Cardiovascular Sciences, UCL, 16-18 Westmoreland Street, London W1G 8PH, UK. Tel: +44 207 573 8888, Fax: +44 207 573 8847, Email: pier.lambiase@uclh.nhs.uk (P.D.L.; human data.); Room1.02, William Harvey Heart Centre, Barts & The London School of Medicine & Dentistry, Charterhouse Square, London EC1M 6BQ, UK. Tel: +44 20 7882 5783, Email: a.tinker@qmul.ac.uk, a.tinker@ucl.ac.uk (A.T.; murine data)

Introduction

Arrhythmogenic right ventricular (RV) cardiomyopathy (ARVC) is a primary heart muscle disorder characterized by a high incidence of ventricular arrhythmias. Early in the disease's course, before the manifestation of RV myocyte loss and fibro-fatty replacement, there is a sub-clinical 'concealed phase'. This presents a major diagnostic and clinical management challenge because arrhythmias and sudden death may arise in the absence of significant clinical and pathological changes.[1] The recent identification of specific desmosomal protein mutations in up to 40% of ARVC patients provides an opportunity to study the pathophysiology of ARVC, specifically whether delayed conduction and a pro-arrhythmic substrate occur in the absence of significant fibrosis.[2]

Abnormal desmosomal proteins are known to be associated with reduced gap junctional Connexin 43 (Cx43) expression which may adversely affect cardiomyocyte electrical coupling. However, there is considerable conduction reserve in ventricular myocardium such that a 95% downregulation in Cx43 reduces transverse conduction velocity (CV) by only 15% and longitudinal conduction by 58%.[3] This has prompted a search for other factors implicated in maintaining conduction reserve which may exert deleterious pro-arrhythmic effects. It has been posited that desmosomal proteins also directly interact with ion channels at the intercalated disc.[4,5] Plakophilin-2 (PKP2) and the sodium (Na) channel, $Na_v1.5$, not only interact but reduced PKP2 expression leads to reduced Na current peak density and altered channel kinetics as well as significant reductions in CV in cultured rat neonatal cardiomyocytes, suggesting that ion channel function is disrupted in some forms of ARVC.[4] However, this has not been demonstrated in any other model or in human disease. We hypothesized that if ARVC begins primarily in the desmosome and alters gap junction coupling, then the sub-clinical manifestations of disease may be identified electrophysiologically prior to histological change. We tested this hypothesis in a murine model with conditional genetic deletion of one allele of desmoplakin (DSP) in the adult heart (DSP $\pm$) and compared the findings with patients carrying desmoplakin mutations.

Methods

Murine

Generation of genetically modified mice

Animals were cared for according to the Animals (Scientific Procedures) Act 1986 (PPL 70/6732). Desmoplakin heterozygotic mice and littermate controls were generated (see Supplementary Material) and studied at 2 and 6 months of age to investigate whether electrophysiological changes occur before overt structural anomalies.[6,7]

Electrophysiological studies, conduction curves, and echocardiography

Mice were anaesthetized with 1.5% isoflurane and a lead II ECG was recorded (Powerlab and Chart software; AD Instruments, Oxford). A 1.1F octapolar electrophysiology catheter (model EPR-801, Millar Instruments) was inserted into the right atrium and ventricle via the jugular vein. The intracardiac electrograms were filtered between 5 and 500 Hz. Pacing stimuli were delivered using the S88 stimulator (Grass Technologies, USA). Electrophysiology studies, similar to clinical studies, were performed as previously described.[8] Pacing output was set at twice diastolic threshold. Sinus node recovery time (SNRT) was calculated by atrial pacing at a cycle length of 100 ms for 15 s. Atrioventricular nodal effective refractory period (AVNERP) was calculated with an atrial drive train at 100 ms and an S2 at 90 ms reduced in 2 ms decrements until AV block occurred. Right ventricular effective refractory period (VERP) was calculated using a ventricular drive train at 100 ms and S2 at 70 ms decreased in 2 ms decrements to refractoriness. Ventricular tachycardia (VT) stimulation was performed with a drive train at 100 ms with up to three extrastimuli (S2, S3, S4) coupled at 70 ms. These were decremented until S2 was refractory. Ventricular tachycardia was defined as greater than 3 beats of broad complex tachycardia exhibiting AV dissociation on the intracardiac electrograms. Mean increase in delay was calculated by dividing the integrated increase in delay by the interval between the basic cycle length and the ventricular refractory period.[9]

Murine histology/immunostaining

Thin sections of myocardial tissue were stained with H&E and Masson Trichrome to detect fibrosis. For Oil red O staining, sections were fixed in 4% paraformaldehyde, washed in distilled water, stained with Oil red O solution in isopropanol, and rinsed in isopropanol. Immunostaining for plakoglobin, Cx43, Na channel, and other surface markers were performed using the following techniques.[10]

Murine

Frozen myocardial sections (10 μm) were fixed with 4% paraformaldehyde, permeabilized with 0.2% Triton X-100 in TBS, and blocked with the 5% goat serum. They were incubated with mouse monoclonal antibodies against DSP (Progen, Germany), mouse monoclonal antibody against plakoglobin (BD Biosciences Pharmingen), rabbit polyclonal antibody against Cx43 (Invitrogen), or rabbit polyclonal antibody against the sodium channel (Alomone Labs, Jerusalem, Israel) overnight at 4°C. Sections were washed with TBS and fluorescence-labelled secondary antibodies (Cy3 goat anti-rabbit and Cy2 goat anti-mouse, Jackson Immunoresearch, PA, USA) were added for 1 h—they were examined using confocal microscopy. Analyses were performed with anonymization of the tissue slides.

Real-time reverse transcriptase polymerase chain reaction

Quantitative real-time reverse transcriptase polymerase chain reaction (RT–PCR) was performed on mouse hearts using Taqman gene expression assays (Applied Biosystems, see Supplementary Methods). All genes were assayed in triplicate with GAPDH as the housekeeping gene by the 2-ΔΔCt method.

Isolation of murine cardiomyocytes and single cell electrophysiology

Cardiomyocyte isolation and patch clamping to assess Na channel current activity were performed using standard techniques (see Supplementary Methods). Peak current inactivation was assessed by fitting the time-decay with a single exponential using ClampFit10.

Human

Human non-contact mapping studies

Endocardial mapping was performed in 22 patients [DSP mutation positive (DSP+) $n = 10$, control ($n = 12$)]. The control group consisted of patients with supraventricular tachycardia (SVT). They had normal resting and signal averaged ECGs, a structurally normal heart on echocardiography and MRI, and no family history of sudden cardiac death. Informed consent was obtained following local research

ethics committee approval. The non-contact mapping study and pacing protocol were performed after SVT ablation in the control patients. The technique for non-contact mapping in the ventricle has been described in detail elsewhere.[11] The multi-electrode array (*Ensite,* St Jude Medical) was deployed via the left femoral vein in the RV outflow tract (RVOT) (see Supplementary Methods for detailed protocol).

Human genetic testing

Genomic DNA from ARVC patients and family members was extracted from whole blood samples using a commercially available DNA extraction kit (QIAamp DNA Blood mini kit, Qiagen). Index cases were part of a larger patient cohort comprehensively screened for mutations in desmoplakin, plakoglobin, plakophilin-2, desmoglein-2, and desmocollin-2. Primer pairs for DSP exons were designed in flanking intronic sequences and are available on request. Polymerase chain reaction amplification and direct sequencing on an ABI 3130 Genetic Analyzer were performed using standard protocols as previously described.[12–14] A total of 300 unrelated healthy, ethnically matched Caucasian volunteers served as controls.

Human study protocol

All patients were studied in the post-prandial state and had stopped anti-dysrhythmic medications for at least five half-lives. After 3 min of steady-state RV apical pacing at 400 ms, an extrastimulus (S_2) was introduced after a drive train of 10 beats according to a standard S_1–S_2 restitution protocol (see Supplementary Methods). A VT stimulation protocol was also performed (Supplementary Methods). The time from the pacing artefact to electrogram peak negative dV/dt was used as the local activation time (AT). Activation–recovery interval (ARI) was defined as the interval between activation time (AT) and repolarization time (RT) and measured as previously described—the Wyatt method was used to measure ARI durations.[15,16] The maximal slope of the ARI restitution curve (S_{max}) was calculated using the least mean squares method.[17] The RV was divided into 16 anatomical segments and the restitution slopes studied in the segments from the RVOT, RV body, and apex.[16]

Human endocardial regional delay and endocardial local activation delay

Mean increase of delay was calculated as described above.[9] The degree of delay was measured from four segments in the RVOT, the RV body, and apex, respectively. Areas of local activation delay during sinus rhythm were determined using activation gradient quantification as previously described.[16] Where slow conduction occurred on the map (i.e. greatest local activation delay), the three-dimensional position, activation gradient (AG) magnitude, and coefficient of determination (r^2) which is a measure of uniformity of wavefront propagation along the endocardial surface were calculated.

Human fractionation index

Endocardial electrograms were filtered at 0.1–100 Hz with a signal to noise ratio set at 1.4 and the number peaks of the differentiated electrogram signal counted as a measure of Fractionation Index—an analagous method to previously published techniques.[18,19] Fractionated electrograms had greater than two deflections.

The human and murine electrophysiological data were anonymized and analysed blinded to the genetic status using semi-automated signal-processing techniques with human verification of signal quality and the electrophysiological measurements.

Human histology and immunostaining

Myocardial biopsies were obtained from three subjects (5, 8, and 9) and immunostained according to the previously published techniques as described for the murine tissue above.[10]

Statistical analysis

Statistical analysis was performed using GraphPad Prism v4 and SigmaStat ver. 3.11, 2004. Full details of the analysis are provided in Supplementary Material. Two-sided *P*-values less than 0.05 were considered statistically significant.

Results

Murine

Murine model

We generated mice with cardiac haploinsufficiency of desmoplakin by intercrossing mice with the *cre* recombinase under the control of the αMHC promoter and mice with exon 2 of the desmoplakin gene flanked by *lox*P sites. The study mice (αMHC cre+, DSP flx\+) were compared with littermate controls (C57\Bl background). As previously reported, we obtained no mice with the αMHC cre+, flx\flx genotype because of probable embryonic lethality.[20] Genotyping of the DSP (flx\+), cre+, and controls was confirmed by PCR from genomic DNA (*Figure 1A*). Quantitative real-time RT–PCR confirmed that there was an approximately 50% reduction in expression compared with control in the αMHC cre+, DSP flx\+ group (*Figure 1E*).

Murine electrophysiological parameters and response to programmed electrical stimulation

The electrophysiological phenotype at 2 months of age was determined. There were no significant differences in the resting surface ECG and invasive electrophysiological parameters between the αMHC cre+, DSP flx\+ mice and controls (*Figure 1B*, *Table 1*). However, a significantly greater proportion of these mice developed inducible VT [9/11 αMHC cre+, DSP flx\+ vs. 0/10 control, $P = 0.0002$, (*Figure 1C*)]. Furthermore, significant differences in the activation time curve profiles, particularly at shorter coupling intervals, were identified on model fitting (*Figure 1D*) ($P < 0.001$). However, the mean increase in delay data was not statistically different (WT 9.48 ± 1.35 ms/ms vs. MHC cre+, DSP flx\+ 9.89 ± 0.90 ms/ms, $P = 0.8$).

Sodium current in isolated myocytes

One explanation for the slowing of conduction and inducibilty of VT would be changes in Na current density. Thus, Na currents were compared between control and αMHC cre+, DSP flx\+ mice, by using single-cell patch clamping. No difference in the maximum Na currents or SCN5A expression from ventricular cardiomyocytes isolated from control mice or desmoplakin ± littermates were detected (*Figure 1E* and *F*). The I/V relationships of I_{Na} were similar in the two animal groups and the τ of inactivation of I_{Na} was not significantly different (*Figure 1F*).

Echocardiography and histology

Although there was no difference in LV dimensions and function on echocardiography (LVIs/LVId 0.22/0.34 cm vs. 0.2/0.36 cm, $n = 5$ in

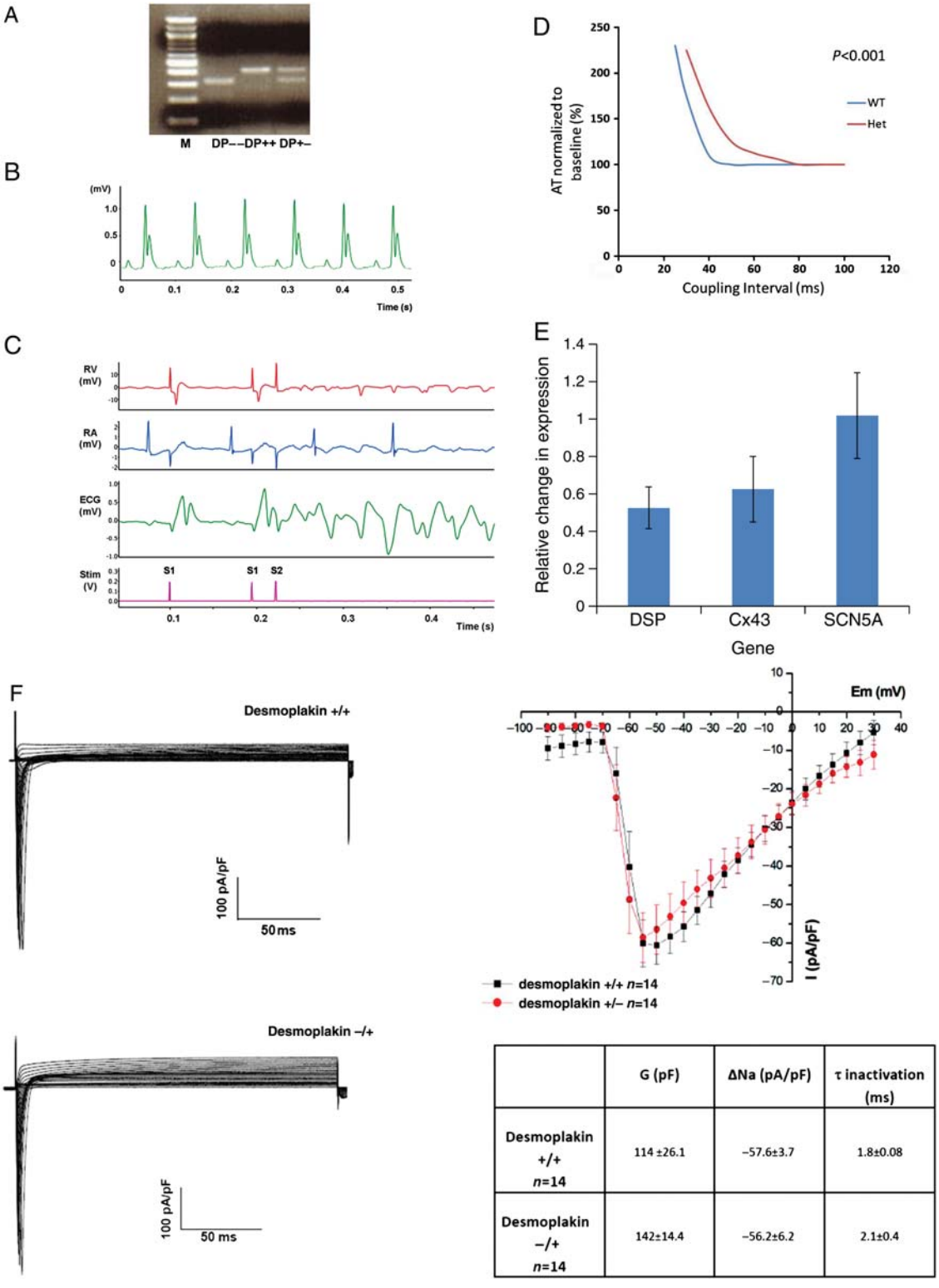

	G (pF)	ΔNa (pA/pF)	τ inactivation (ms)
Desmoplakin +/+ n=14	114 ±26.1	−57.6±3.7	1.8±0.08
Desmoplakin −/+ n=14	142±14.4	−56.2±6.2	2.1±0.4

Figure 1 (*A*) Screening of mouse tail DNA by PCR—the floxed DSP allele gives a 410 bp band and the wild-type (WT) allele gives a 320 bp band. (*B*) Example of a murine surface ECG recording. (*C*) Example of single premature extrastimulus (S2) causing polymorphic ventricular tachycardia. (RA, right atrial intracardiac electrogram; RV, right ventricular intracardiac electrogram; ECG, surface ECG recording; stim, stimulator output). (*D*) Activation time curves (AT) normalized to baseline AT for mice by genotype (AT, activation time) ($n = 10$ WT, $n = 11$ DSP $\pm$). (*E*) Relative mRNA expression by genotype by RT–PCR in 2-month-old desmoplakin ($\pm$) myocytes vs. WT ($n = 10$ WT, $n = 11$ DSP $\pm$). (*F*) Electrophysiology of the Na^+ current using patch–clamp technique: current traces (left), I/V relationships (top right), and electrophysiological parameters (bottom right).

Table 1 Surface ECG and electrophysiological parameters

Interval	WT (ms) ($n = 10$)	SEM (±)	Het KO (ms) ($n = 11$)	SEM (±)	Human SVT control (ms) ($n = 12$)	SEM (±)
RR	114	3	110	3.9	760	38
PR	38	0.8	38	1.1	146	27
QTc	23	0.9	24	1.6	374	50
QRS	9	0.1	10	0.3	90	4
SNRT	121	6.5	113	6.2		
cSNRT	21	4	16	3.1		
AVW	57	3.1	58	3.1	302	35
AV 2:1	45	2.4	48	2.8		
AVNERP	46	3.2	45	3.5	250	30
VERP	34	3.2	27	3.2	212	6
VT duration			2229	606		
VT CL			37	3.1		

each group) (*Figure 2A*), there was evidence of slippage of individual myocardial strands in the RV sections of the αMHC cre+, DSP flx\+ mice but no change in left ventricular sections (*Figure 2B*). Importantly, there was no evidence of replacement of myocytes with fibro-fatty tissue and interstitial fibrosis in 2-month-old mice who underwent EP studies (*Figure 2B*). However, in 6-month-old mice, focal myocyte loss and fibro-fatty replacement are observed, showing that DSP αMHC cre+, DSP flx\+ mice do develop histological abnormalities with time (*Figure 2B* and *C*)). A second explanation for the slowed CV would be changes in Cx43.

Immunohistochemistry in 2-month-old mice demonstrated reductions in Cx43 signal as corroborated by quantitative real-time RT–PCR (*Figure 1E*) and less co-localization with β-catenin, forming cytoplasmic aggregates of Cx43. β-Catenin was used as a marker of the intercalated disk and its' signal and localization remained constant between the genotypes; therefore, there was less Cx43 at the intercalated disk (*Figure 3A*). $Na_v1.5$ was found at the disk, in the endoplasmic reticulum and on the actin filaments (*Figure 3B*). It did not show any reduction in signal or change in localization in the α MHC cre+, DSP flx\+ animals. There was no change in the localization of plakoglobin in the mice that underwent electrophysiology studies (*Figure 3C*). DSP signal at the intercalated disk was reduced in αMHC cre+, DSP flx\+ mice (*Figure 3D*). However, 6-month-old mice did show reduced levels of DSP and a small reduction in plakoglobin signal at the intercalated disks (*Figure 3E* and *F*).

Human

Patient characteristics

The demographics and clinical features of the DSP study subjects are shown in *Table 2*; mean age was 44(±15) years. These patients had been identified in families with desmoplakin mutations and a clinical diagnosis of ARVC based upon the most recent Task Force criteria, with 5/10 having a definite diagnosis, 4/10 borderline, and possible in 1/10.[21–25] The patients had well preserved left ventricular function except one subject (no. 5) who had an ejection fraction of 40%. No other patients had significant RV or LV wall motion abnormalities meeting ARVC Task Force Criteria. Seven DSP patients received an ICD, one received post-VF arrest, and six received secondary prevention due to a history of unexplained syncope (3) or documented VT in the context of family history of sudden cardiac death (2)/impaired left ventricular function (1). Three patients received appropriate ICD shock therapies (mean FUp 72 months) (see Supplementary material online, *Table S1* for further details). The 12 control subjects with SVT (no history of atrial fibrillation, *Table 1* shows baseline electrophysiological characteristics) and structurally normal hearts had an equivalent mean age of 44 (±21) years and sex distribution (3M:9F).

Isochronal mapping to identify the site of maximal delay

Figure 4 illustrates the isochronal maps recorded during RV apical pacing at 400 ms obtained from a control and DSP mutation carrier (DSP+). There is clearly a more prolonged RV depolarization in the DSP+ patient. However, in the group data, mean endocardial activation time in patients with DSP disease was not significantly different from controls either in sinus rhythm (41 ± 8 vs. 40 ± 5 ms in controls) or with steady-state RV apical pacing at 400 ms cycle length (42 ± 13 vs. 42 ± 8 ms).

Quantification of regional and local conduction delay

Employing an alternative well-validated method to quantify the extent of regional conduction delay and inhomogeneity,[26,27] no significant reductions in activation gradient at the site of slowest conduction in sinus rhythm were identified in DSP mutation carriers [0.4 ± 0.1 mm/ms in DSP+ patients vs. 0.47 ± 0.15 mm/ms in control patients (P = ns)]. The uniformity of wavefront propagation as measured by r^2 was 0.98 ± 0.02 for DSP+ patients vs. 0.94 ± 0.04 for controls ($P < 0.05$).

However, on multiple regression analysis, overall DSP+ patients' hearts had significantly more prolonged AT restitution curve profiles vs. controls at CI < 250 ms ($P < 0.001$) (see Supplementary material online, *Figure S1*). These delays were also significantly different in each of the three RV regions—RVOT, body, and apex between the DSP mutation carriers and controls ($P < 0.001$ per region). Furthermore, statistically significant regional

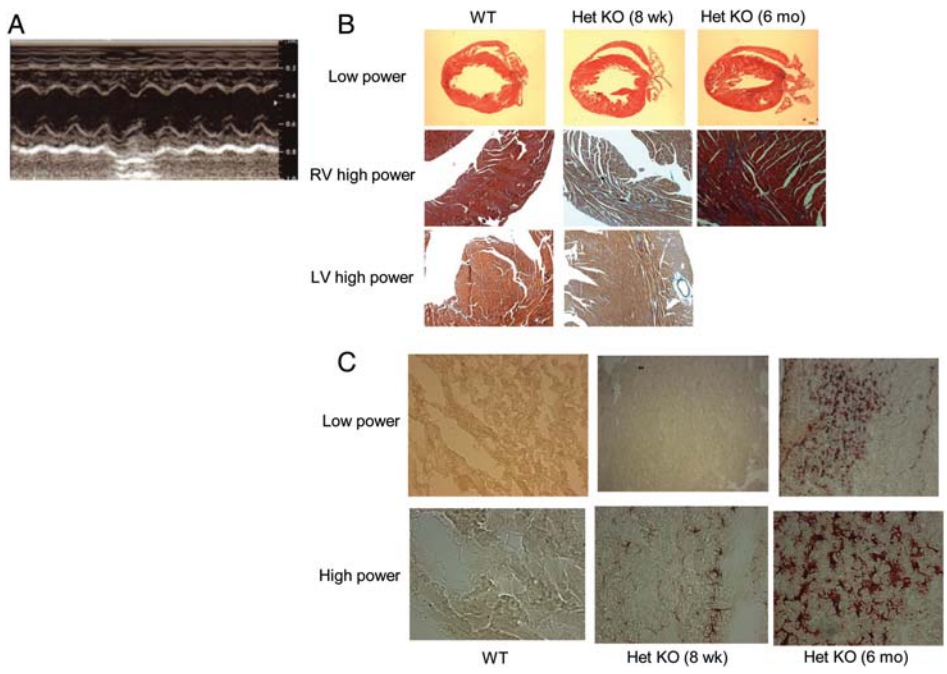

Figure 2 (*A*) M-mode echocardiogram of a desmoplakin (±) mouse. (*B*) Histological features of DSP het KO mice (Masson's trichrome stain) illustrating fibrosis in 6-month-old DSP± stained in blue. (*C*) Oil red O staining in 8-week and 6-month-old Het KO mice illustrating accumulation of fat droplets with age.

conduction delays occurred in the RVOT measuring 38% greater than controls (*Figure 4B*). This corresponds to the delayed activation time profiles in the DSP± mice.

Fractionation of electrograms and endocardial activation–recovery interval restitution curves

Applying the definition of fractionation stated above, DSP+ hearts had a significantly greater degree of fractionation vs. controls and was most marked in the RVOT (*Figure 5A–C*). *Figure 5* demonstrates this regionality of fractionation in subject 8, illustrating examples of electrogram morphology in RVOT and apical sites compared with equivalent sites in controls.

The mean ARI of all the segmental restitution curves at 400 ms baseline cycle length in the DSP + RV and control RV during RV apical pacing were compared (*Figure 5D–F*). Analysis of all the curves by model fitting and testing for interaction confirmed significant differences in the ARI at RVOT, RV body vs. apex in DSP+ patients at both long and short coupling intervals (CI's) which did not occur in controls. In control subjects, the ARI curves show a significant ARI prolongation only in the RVOT when compared with the apex over a large range of CI's ($P < 0.001$), but the mean RV body ARI curves were similar to the apex (*Figure 5D*). However, in the DSP+ patients, the RV body and RVOT both had significantly greater ARI prolongation than the apex ($P < 0.001$).

Not only were there differences between regions in the DSP+ group data, differences in the ARI restitution curves could be identified between equivalent RV regions in the patient populations. As seen in *Figure 5D*, the ARI curves in control subjects show a profile in which they maximize and then curve downwards with increasing CI's. This profile was similar at the RVOT, body, and the apex. However, in the DSP+ group, the curves at the apex, RV body, and RVOT were more linear in this range of CI's. The ARI values for any given coupling interval were longer in the RV body and RVOT for DSP+ patients vs. the same regions in controls ($P < 0.001$) (*Figure 5E* and *F*). This indicates that there is a large interval dependent dispersion of ARI in the DSP+ patients. The maximal slopes of ARI restitution curves were compared between control and DSP+ subjects. The odds of having a segment with a $S_{max} > 1$ was 99% higher (95% CI: 13%; 351%, $P = 0.017$) in the DSP+ group.

Immunohistochemistry of human biopsies

One patient had impaired LV function (no. 5) and underwent RV biopsy. There was no evidence of fibro-fatty replacement, but plakoglobin and desmosmal Cx43 expression was downregulated (*Figure 6A*). In two other cases without cardiac imaging anomalies, RV biopsies showed that Na_v 1.5 was localized away from the intercalated disk, marked by β-catenin, aggregating in the cytoplasm of the myocytes (subject 8, *Figure 6B* (i)) or on the actin filaments (subject 9, *Figure 6B* (ii)). This differs from the absence of Na channel mislocalization identified in the DSP± mice.

Discussion

The principle findings in the DSP± mice include (i) evidence of slow conduction at short coupling intervals and inducibilty of VT

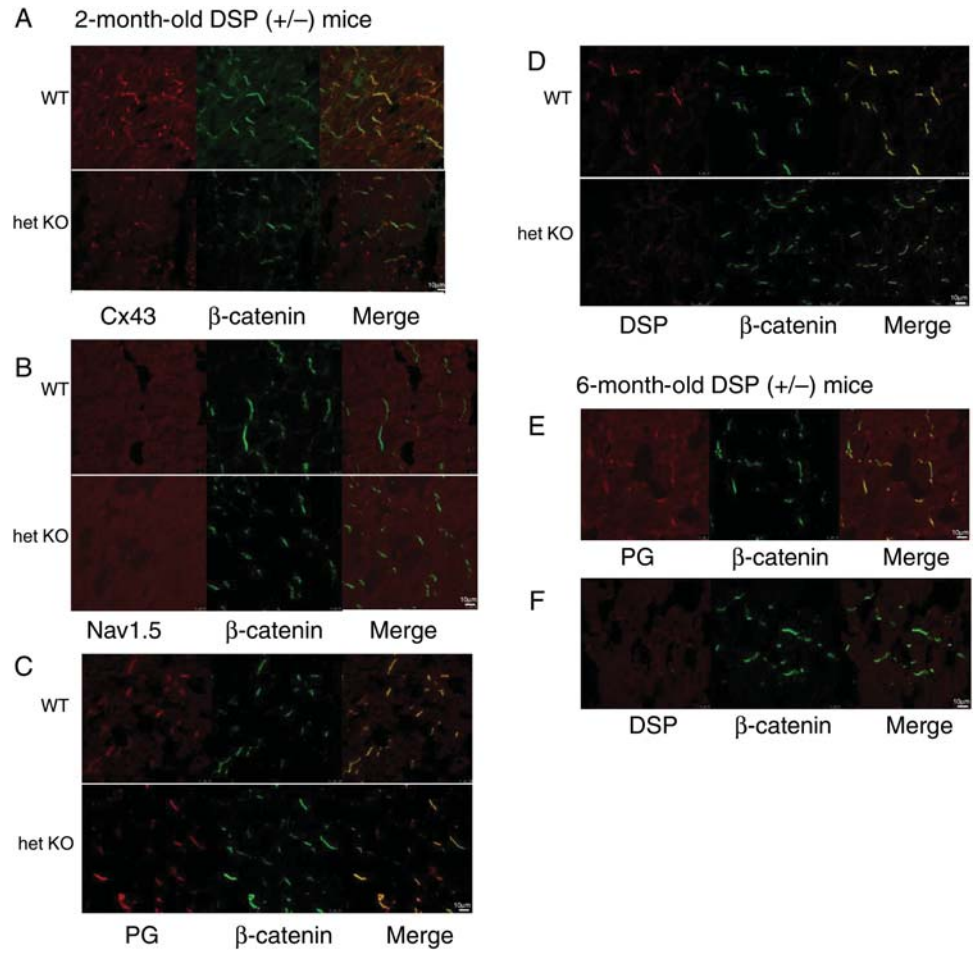

Figure 3 Representative immunofluorescence images of murine ventricular myocardium. (*A*) Cx43, (*B*) Nav1.5, (*C*) Plakoglobin (PG), (*D*) DSP labelling, all 8-week-old mice. (*E*) Plakoglobin and (*F*) DSP immunohistochemistry from 6-month-old mice. $n=4$ per genotype with consistent staining in each mouse.

and (ii) a subtle histological substrate with mislocalization and reduced intercalated disc expression of Cx43 in the absence of fibro-fatty changes at 2 months of age but preserved Na channel activity on patch clamping. Similarly, in human desmoplakin mutation carriers, there was significant conduction delay at short coupling intervals with no evidence of fibro-fatty replacement, but desmosmal Cx43 expression was also downregulated with some evidence of Na channel mislocalization. The major novel findings in this study are that electrophysiological abnormalities occur *prior* to major structural changes such as fibrosis in both the human disease and a murine model. Secondly, this occurs because of slowed conduction due to a mislocalization and a reduction in expression of Cx43.

Murine models of arrhythmogenic right ventricular cardiomyopathy

We investigated early electrophysiological changes in a cardiac haploinsufficient desmoplakin murine model. Ventricular tachycardia was readily induced together with conduction delay prior to the structural changes revealed by echocardiography and conventional histology. This conduction delay was coupled with reduced intercalated disc Cx43 localization. Na channels were not mislocalized away from the sarcolemma as supported by patch clamping. Thus, haploinsufficiency of desmoplakin is sufficient to result in Cx43 mislocalization, conduction slowing, and an arrhythmic phenotype. In a previous study on a similar model, it was concluded that nuclear localization of plakoglobin suppressed Wnt/beta-catenin signalling and fibro-fatty replacement developed due to changes in myocyte gene expression.[28,29] The electrophysiological phenotype was not examined before overt pathological changes occurred. In the only published murine model of clinical DSP mutations, a transgenic mouse expressing the C-terminal mutation R2834H had major structural anomalies. Cx43 and plakoglobin were redistributed to the detergent soluble fraction of the heart cell lysate, but electrophysiological assessment was not performed.[30] In plakoglobin-deficient mice, there were no detectable structural histological or Cx43 abnormalities. However, prolonged RV activation time, increased ventricular ectopic burden, and RV dilatation were associated with increased age and training.[31]

Table 2 Patient demographics

Subject no.	Age (M/F)	Mutation	RV structural abnormalities	TW inversion V1–V3	Small QRS complex	S wave delay (>55 ms)	SAv ECG	NSVT	SVT	PVCs >500/24 h	Inducible VT at EP study	FHx	ICD	Criteria Maj/Min
1	43 F	E274fsX288[25]	–	–	+	–	–	+	+	+	–	–	+	1/1
2	50 F	S507F[23]	–	–	+	–	–	+	–	+	–	Major	+	1/1
3	61 F	T586fsx594[22]	–	+	–	–	–	–	–	–	–	Minor	+	1/0
4	28 F	T586fsx594[22]	–	–	–	–	–	+	–	–	–	Major	+	1/1
5	72 F	S507F[23]	LV EF 40%	–	–	+	+	–	–	+	–	Major	+	1/2
6	53 F	T586fsx594[22]	–	+	–	–	+	–	–	–	–	–	+	2/1
7	37 M	E274fsX288[25]	–	–	–	–	+	+	–	–	–	+	–	1/2
8	22 M	S922fsX928[24]	–	–	–	–	+	+	–	–	+	–	+	1/2
9	40 F	N408K and R941X[a]	–	–	–	+	+	+	–	–	–	Major	–	1/2
10	33 M	T586fsx594[22]	–	–	–	–	–	+	–	+	–	Major	–	1/1

[a]Leads to a premature stop codon and protein truncation.

Transgenic mice with cardiac restricted expression of a clinically identified desmoglein-2 gene mutation (N271S) recapitulated clinical features including spontaneous ventricular arrhythmias and sudden death, cardiac dysfunction, biventricular dilatation, and ventricular aneurysms. However, such models overexpress mutant alleles which are not seen in the clinical situation. Again, a detailed characterization of the cardiac electrophysiology remains to be undertaken.[32] Therefore, the majority of murine ARVC models demonstrate a profound structural phenotype and the arrhythmic burden has been studied in this context. Uniquely, we demonstrate that an electrophysiological substrate exists due to conduction slowing and Cx43 mislocalization prior to major structural and histological changes.

Sodium channel effects

In the human biopsy samples, the Na channel appeared to localize to the intercalated disc in one patient, while in another it was retained intracellularly and might potentially contribute to a reduced CV. A potential reason for the difference between the murine model where no changes in Na channel activity occurred and man is human mutations may have a different genetic mechanism from simple haploinsufficiency, e.g. missense mutations could result in gain-of-function or dominant-negative effects. Therefore, such mechanisms could result in a more severe cellular lesion which might additionally involve the Na channel.

Human mapping studies in arrhythmogenic right ventricular cardiomyopathy

In an analogous manner, previous clinical electrophysiological mapping studies in ARVC examined patients with advanced disease where structural abnormalities were evident on conventional imaging. Both Corrado *et al.*[33] and Calkins and co-authors[34] have demonstrated fractionation and conduction delay, respectively. However, these studies were conducted mainly in non-genotyped patients who fulfilled Task Force Criteria with advanced structural disease, for example in Corrado's population, 81% had RV wall motion abnormalities. Furthermore, voltage mapping alone may miss areas containing less than 40% fibro-fatty endocardial tissue replacement.[35] Gadolinium enhanced MRI is even less sensitive missing 91% of scar with $<$20% RV area.[36] Our study of DSP mutation carriers confirms that not only does conduction delay and electrogram fractionation develop early in this form of ARVC before detectable cardiac imaging abnormalities, but it can precede overt histological changes. These conduction delays only became evident with shorter coupling intervals, demonstrated by the activation delay curves, particularly in the RVOT. This can be explained by a number of factors affecting propagation in the RV, including variable path length at shorter coupling intervals, a change from longitudinal to transverse conduction, wave front curvature, differences in gap junction distribution, and channel kinetics. The increased fractionation could be explained by dissociation of the myocyte layers as heterogeneity in gap junction distribution and early fibrosis will promote discontinuous myocardial conduction pathways. A similar pattern was observed in the cardiac desmoplakin haploinsufficient mice which had delayed

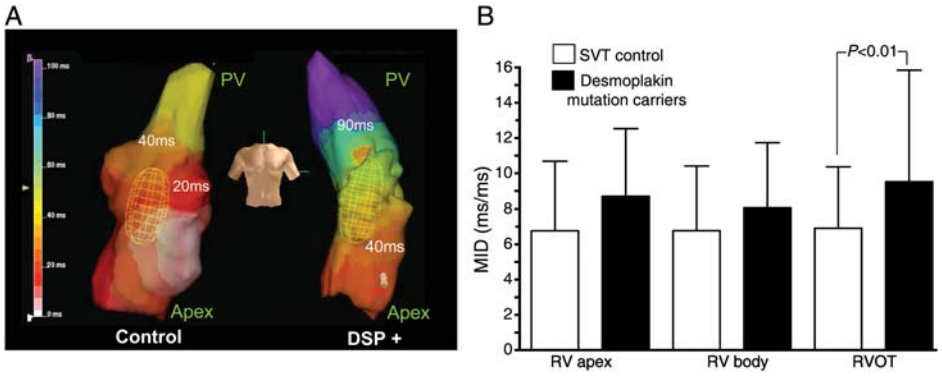

Figure 4 (*A*) Isochronal map showing RV activation sequence with steady-state pacing from RV apex at 400 ms cycle length (subject 5 vs. control). PV, pulmonary valve. (*B*) Mean increase delay according to the region in DSP+ and control groups.

conduction but only at shorter coupling intervals compared with controls. Thus, increased stress on myocardial conduction was required to demonstrate differences in the conduction reserve of the tissue most probably due to the less overt structural changes. Only as the disease transitions to more extensive fibro-fatty replacement then do activation gradients and RV activation times become more prolonged at long coupling intervals and at resting heart rates when conduction reserve diminishes further, consistent with the findings of the Calkins group.[34]

Our human mapping data also demonstrated additional regional electrophysiological abnormalities that are difficult to investigate in the mouse. Significantly prolonged ARI's were identified in the RVOT and RV body even at short coupling intervals, a function of the fact that conduction delay in these regions most probably prevented engagement of the proximal portion of the ARI restitution curve in these segments. These apical–basal gradients in ARI particularly in the RV body would create ideal conditions for conduction block and re-entry at both resting and increased heart rates, therefore increasing the probability of ventricular arrhythmia. Interestingly, despite the more marked conduction delay, the probability of a DSP+ patient's RV having an $S_{max} > 1$ was increased, indicating that the substrate was more likely to promote wave break and VF. This has important implications since it is well recognized that sudden cardiac death can occur in patients with minimal histological changes in the sub-clinical phase of ARVC and thus a more sophisticated clinical phenotyping approach examining these dynamic conduction–repolarization changes is required.

Clinical implications

These data may also explain the early phase of the disease when ventricular tachyarrhythmias and sudden death occur at short coupling intervals during stress, exercise, or sports activity (increased adrenergic drive) due to the initial reduction in conduction reserve and steep S_{max}. In contrast, during later phases of ARVC when demonstrable structural changes ensue (fibrosis and myocyte atrophy), ventricular arrhythmias are more common at rest as a monomorphic VT. The advanced structural changes promote greater conduction delay at longer coupling intervals to prevent engagement of the proximal portion of the ARI restitution curve reducing the possibility of VT degenerating into VF which occurs in the early subclinical phase. Therefore, the ventricular arrhythmias in ARVC may arise from different mechanisms as the disease progresses with the development of structural changes over time.

The early manifestations of ARVC are subclinical, escaping detection on conventional imaging and the surface ECG. In this study of desmoplakin disease, subclinical electrophysiological effects precede any overt structural changes in a murine model and in patients. High-density electrophysiological mapping of the substrate in cases with suspected ARVC may reveal differences in conduction and repolarization kinetics to aid identification of cases where close monitoring is indicated for disease progression.

Study limitations

The human mapping technique evaluates endocardial electrophysiology and thus mid-myocardial and epicardial effects of DSP disease could not be assessed. This is important since mapping studies suggest that structural changes manifest epicardially prior to progressing endocardially. It was not possible to perform high-density mapping *in vivo* in the murine model, a technique requiring further development since this would provide more physiological data in the innervated murine heart as opposed to current techniques which generally utilize a unloaded, denervated Langendorff preparation. The qPCR and immunohistochemical results showing down regulation in Cx43 could not be verified by western blotting since we were not convinced that the specified commercial antibody was appropriately detecting the protein. However western blotting for Cx43 has been shown to be more sensitive than immunostaining in other models.[37]

There was only limited human biopsy material available to study Na channel distribution in the patients. These observations need to be verified in a larger cohort.

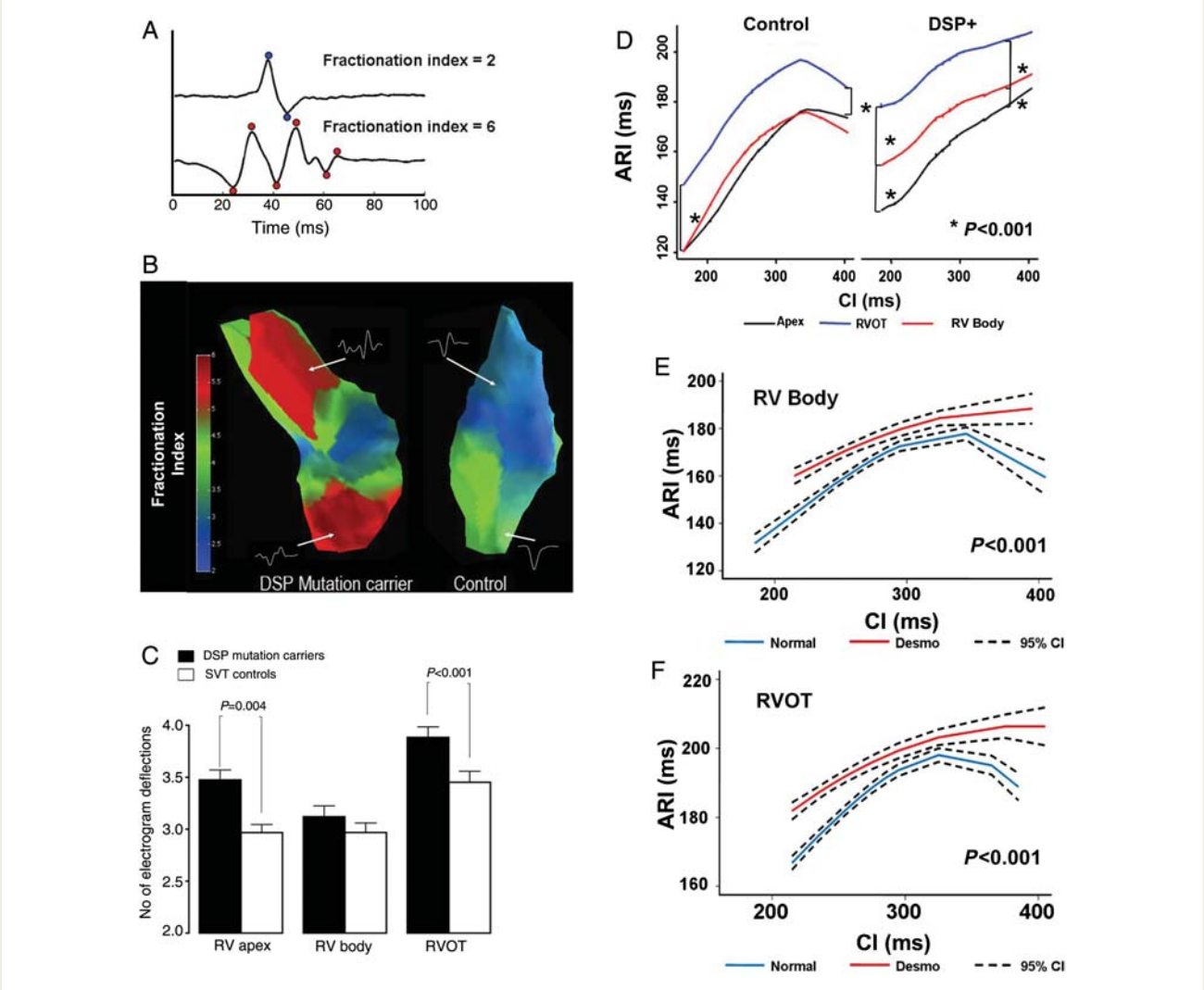

Figure 5 (*A*) Example of normal and fractionated EGMs analysed using fractionation index algorithm. (*B*) Fractionation index (FI) map illustrating degree of electrogram fractionation in RV segments. Colour scale represents the FI for sites sampled on the RV endocardium. (*C*) Histogram illustrating mean FI (no of deflections per EGM) according to the region in DSP+ and control subjects. (*D*) Mean ARI restitution curves recorded from the apex, RV body, and RVOT in control and DSP+ groups. (*E*) Mean ARI curves in control and DSP+ subjects in the RV body and (*F*) RVOT.

Conclusion

Abnormalities in desmoplakin expression in a murine model and human desmoplakin mutation carriers result in significant changes in conduction and repolarization kinetics prior to structural changes. The data support the view that ARVC is a desmosomal disease caused by desmosomal protein mutations affecting myocyte electrical coupling, primarily Cx43 mislocalization, and promoting structural changes as the disease progresses through different phases. Cx43 mislocalization is sufficient and central to the development of an arrhythmic phenotype. The clinical detection of these early electrophysiological manifestations using high-density mapping of conduction–repolarization characteristics has important implications both in the earlier diagnosis of ARVC before structural changes become evident and improved risk stratification of this challenging condition.

Supplementary material

Supplementary material is available at *European Heart Journal* online.

Funding

Funding was provided by British Heart Foundation, Department of Health's NIHR Biomedical Research Centres funding scheme support to UCLH and UCL, Educational Grant St Jude Medical and the Stephen Lyness Research Fund. Funding to pay the Open Access publication charges for this article was provided by the Wellcome Trust.

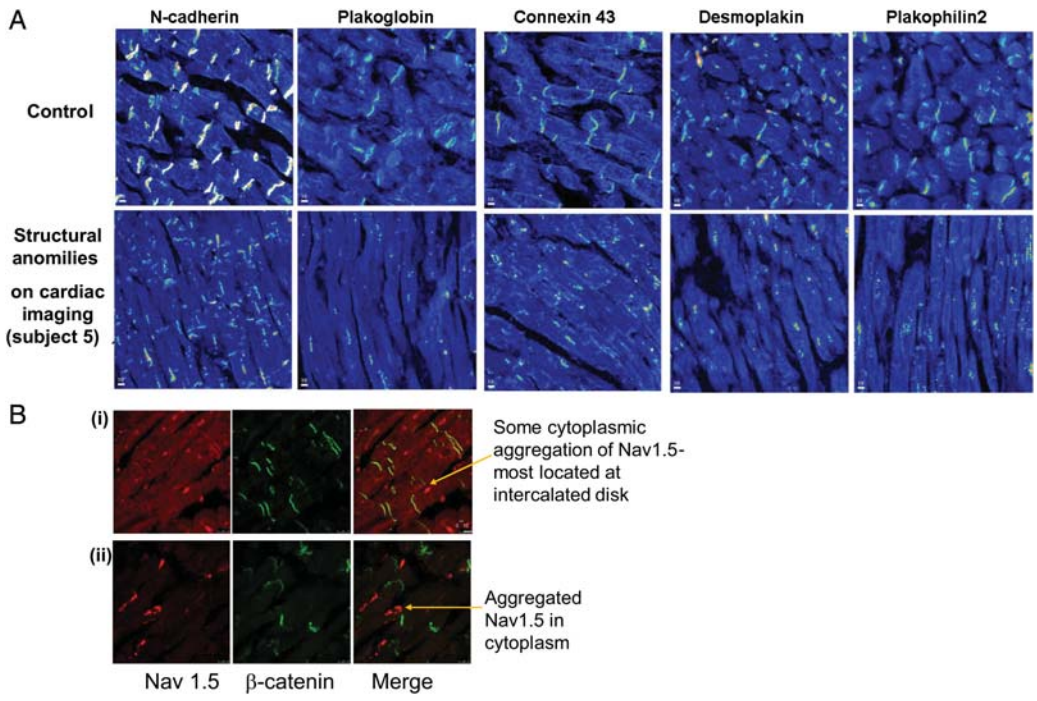

Figure 6 Human histology. (*A*) Expression of N-cadeherin (intercalated disc marker protein), Cx43, and plakoglobin in subjects 5 (with LV impairment on imaging). (*B*) Immunofluorescence images of Nav1.5 expression in two subjects (8 and 9) without structural changes on cardiac imaging.

Conflict of interest: M.F. receives an educational grant from St Jude Medical.

References

1. Kaplan SR, Gard JJ, Protonotarios N, Tsatsopoulou A, Spiliopoulou C, Anastasakis A, Squarcioni CP, McKenna WJ, Thiene G, Basso C, Brousse N, Fontaine G, Saffitz JE. Remodeling of myocyte gap junctions in arrhythmogenic right ventricular cardiomyopathy due to a deletion in plakoglobin (Naxos disease). *Heart Rhythm* 2004;**1**:3–11.
2. Saffitz JE. Arrhythmogenic cardiomyopathy and abnormalities of cell-to-cell coupling. *Heart Rhythm* 2009;**6**(8 suppl):S62–S65.
3. van Rijen HV, Eckardt D, Degen J, Theis M, Ott T, Willecke K, Jongsma HJ, Opthof T, de Bakker JM. Slow conduction and enhanced anisotropy increase the propensity for ventricular tachyarrhythmias in adult mice with induced deletion of connexin43. *Circulation* 2004;**109**:1048–1055.
4. Sato PY, Musa H, Coombs W, Guerrero-Serna G, Patiño GA, Taffet SM, Isom LL, Delmar M. Loss of plakophilin-2 expression leads to decreased Na current and slower conduction velocity in cultured cardiac myocytes. *Circ Res* 2009;**105**:523–526.
5. Delmar M, McKenna WJ. The cardiac desmosome and arrhythmogenic cardiomyopathies: from gene to disease. *Circ Res* 2010;**107**:700–714.
6. Vasioukhin V, Bowers E, Bauer C, Degenstein L, Fuchs E. Desmoplakin is essential in epidermal sheet formation. *Nat. Cell Biol* 2001;**3**:1076–1085.
7. Agah R, Frenkel PA, French BA, Michael LH, Overbeek PA, Schneider MD. Targeted expression of Cre recombinase provokes cardiac-restricted, site-specific rearrangement in adult ventricular muscle in vivo. *J Clin Invest* 1997;**100**:169–179.
8. Berul CI, Christe ME, Aronovitz MJ, Seidman CE, Seidman JG, Mendelsohn ME. Electrophysiological abnormalities and arrhythmias in alpha MHC mutant familial hypertrophic cardiomyopathy mice. *J Clin Invest* 1997;**99**:570–576.
9. Kawara T, Derksen R, de Groot JR, Coronel R, Tasseron S, Linnenbank AC, Hauer RN, Kirkels H, Janse MJ, de Bakker JM. Activation delay after premature stimulation in chronically diseased human myocardium relates to the architecture of interstitial fibrosis. *Circulation* 2001;**104**:3069–3075.
10. Asimaki A, Tandri H, Huang H, Halushka MK, Gautam S, Basso C, Thiene G, Tsatsopoulou A, Protonotarios N, McKenna WJ, Calkins H, Saffitz JE. A new diagnostic test for arrhythmogenic right ventricular cardiomyopathy. *N Engl J Med* 2009;**360**:1075–1084.
11. Schilling RJ, Davies DW, Peters NS. Characteristics of sinus rhythm electrograms at sites of ablation of ventricular tachycardia relative to all other sites: a noncontact mapping study of the entire left ventricle. *J Cardiovasc Electrophysiol* 1998;**9**:921–933.
12. Syrris P, Ward D, Asimaki A, Sen-Chowdhry S, Ebrahim HY, Evans A, Hitomi N, Norman M, Pantazis A, Shaw AL, Elliott PM, McKenna WJ. Clinical expression of plakophilin-2 mutations in familial arrhythmogenic right ventricular cardiomyopathy. *Circulation* 2006;**113**:356–364.
13. Syrris P, Ward D, Evans A, Asimaki A, Gandjbakhch E, Sen-Chowdhry S, McKenna WJ. Arrhythmogenic right ventricular dysplasia/cardiomyopathy associated with mutations in the desmosomal gene desmocollin-2. *Am J Hum Genet* 2006;**79**:978–984.
14. Syrris P, Ward D, Asimaki A, Evans A, Sen-Chowdhry S, Hughes SE, McKenna WJ. Desmoglein-2 mutations in arrhythmogenic right ventricular cardiomyopathy: a genotype-phenotype characterization of familial disease. *Eur Heart J* 2007;**28**:581–588.
15. Yue AM, Franz MR, Roberts PR, Morgan JM. Global endocardial electrical restitution in human right and left ventricles determined by noncontact mapping. *J Am Coll Cardiol* 2005;**46**:1067–1075.
16. Yue AM, Betts TR, Roberts PR, Morgan JM. Global dynamic coupling of activation and repolarization in the human ventricle. *Circulation* 2005;**112**:2592–2601.
17. Taggart P, Sutton P, Chalabi Z, Boyett MR, Simon R, Elliott D, Gill JS. Effect of adrenergic stimulation on action potential duration restitution in humans. *Circulation* 2003;**107**:285–289.
18. Lambiase PD, Ahmed AK, Ciaccio EJ, Brugada R, Lizotte E, Chaubey S, Ben-Simon R, Chow AW, Lowe MD, McKenna WJ. High density substrate mapping in Brugada syndrome—combined role of conduction and repolarization heterogeneities in arrhythmogenesis. *Circulation* 2009;**120**:106–117, 1–4.
19. Postema PG, van Dessel PF, de Bakker JM, Dekker LR, Linnenbank AC, Hoogendijk MG, Coronel R, Tijssen JG, Wilde AA, Tan HL. Slow and discontinuous conduction conspire in Brugada syndrome: a right ventricular mapping and stimulation study. *Circulation* 2008;**1**:379–386.

20. Gallicano GI, Kouklis P, Bauer C, Yin M, Vasioukhin V, Degenstein L, Fuchs E. Desmoplakin is required early in development for assembly of desmosomes and cytoskeletal linkage. *J Cell Biol* 1998;**143**:2009–2022.
21. Marcus FI, McKenna WJ, Sherrill D, Basso C, Bauce B, Bluemke DA, Calkins H, Corrado D, Cox MG, Daubert JP, Fontaine G, Gear K, Hauer R, Nava A, Picard MH, Protonotarios N, Saffitz JE, Sanborn DM, Steinberg JS, Tandri H, Thiene G, Towbin JA, Tsatsopoulou A, Wichter T, Zareba W. Diagnosis of arrhythmogenic right ventricular cardiomyopathy/dysplasia: proposed modification of the task force criteria. *Circulation* 2010;**121**:1533–1541.
22. Norman M, Simpson M, Mogensen J, Shaw A, Hughes S, Syrris P, Sen-Chowdhry S, Rowland E, Crosby A, McKenna WJ. Novel mutation in desmoplakin causes arrhythmogenic left ventricular cardiomyopathy. *Circulation* 2005;**112**:636–642.
23. Sen-Chowdhry S, Syrris P, McKenna WJ. Role of genetic analysis in the management of patients with arrhythmogenic right ventricular dysplasia/cardiomyopathy. *J Am Coll Cardiol* 2007;**50**:1813–1821.
24. Elliott P, O'Mahony C, Syrris P, Evans A, Rivera Sorensen C, Sheppard MN, Carr-White G, Pantazis A, McKenna WJ. Prevalence of desmosomal protein gene mutations in patients with dilated cardiomyopathy. *Circ Cardiovasc Genet* 2010;**3**:314–322.
25. http://arvcdatabase.info/mutationdetails.
26. Ciaccio EJ, Chow AW, Davies DW, Wit AL, Peters NS. Localization of the isthmus in reentrant circuits by analysis of electrograms derived from clinical noncontact mapping during sinus rhythm and ventricular tachycardia. *J Cardiovasc Electrophysiol* 2004;**15**:27–36.
27. Ciaccio EJ. Localization of the slow conduction zone during reentrant ventricular tachycardia. *Circulation* 2000;**102**:464–469.
28. Conacci-Sorrell M, Zhurinsky J, Ben-Ze'ev A. The cadherin-catenin adhesion system in signaling and cancer. *J Clin Invest* 2002;**109**:987–991.
29. Garcia-Gras E, Lombardi R, Giocondo MJ, Willerson JT, Schneider MD, Khoury DS, Marian AJ. Suppression of canonical Wnt/beta-catenin signaling by nuclear plakoglobin recapitulates phenotype of arrhythmogenic right ventricular cardiomyopathy. *J Clin Invest* 2006;**116**:2012–2021.
30. Yang Z, Bowles NE, Scherer SE, Taylor MD, Kearney DL, Ge S, Nadvoretskiy VV, DeFreitas G, Carabello B, Brandon LI, Godsel LM, Green KJ, Saffitz JE, Li H, Danieli GA, Calkins H, Marcus F, Towbin JA. Desmosomal dysfunction due to mutations in desmoplakin causes arrhythmogenic right ventricular dysplasia/cardiomyopathy. *Circ Res* 2006;**99**:646–655.
31. Kirchhof P, Fabritz L, Zwiener M, Witt H, Schäfers M, Zellerhoff S, Paul M, Athai T, Hiller KH, Baba HA, Breithardt G, Ruiz P, Wichter T, Levkau B. Age- and training-dependent development of arrhythmogenic right ventricular cardiomyopathy in heterozygous plakoglobin-deficient mice. *Circulation* 2006;**114**:1799–1806.
32. Pilichou K, Remme CA, Basso C, Campian ME, Rizzo S, Barnett P, Scicluna BP, Bauce B, van den Hoff MJ, de Bakker JM, Tan HL, Valente M, Nava A, Wilde AA, Moorman AF, Thiene G, Bezzina CR. Myocyte necrosis underlies progressive myocardial dystrophy in mouse dsg2-related arrhythmogenic right ventricular cardiomyopathy. *J Exp Med* 2009;**206**:1787–1802.
33. Corrado D, Basso C, Leoni L, Tokajuk B, Bauce B, Frigo G, Tarantini G, Napodano M, Turrini P, Ramondo A, Daliento L, Nava A, Buja G, Iliceto S, Thiene G. Three-dimensional electroanatomic voltage mapping increases accuracy of diagnosing arrhythmogenic right ventricular cardiomyopathy/dysplasia. *Circulation* 2005;**111**:3042–3050.
34. Tandri H, Asimaki A, Abraham T, Dalal D, Tops L, Jain R, Saffitz JE, Judge DP, Russell SD, Halushka M, Bluemke DA, Kass DA, Calkins H. Prolonged RV endocardial activation duration: a novel marker of arrhythmogenic right ventricular dysplasia/cardiomyopathy. *Heart Rhythm* 2009;**6**:769–775.
35. Avella A, D'Amati G, Zachara E, Musumeci F, Tondo C. Comparison between electroanatomic and pathologic findings in a patient with arrhythmogenic right ventricular cardiomyopathy/dysplasia treated with orthotopic cardiac transplant. *Heart Rhythm* 2010;**7**:828–831.
36. Santangeli P, Hamilton-Craig C, Russo AD, Pieroni M, Casella M, Pelargonio G, Biase LD, Smaldone C, Bartoletti S, Narducci ML, Tondo C, Bellocci F, Natale A. Imaging of scar in patients with ventricular arrhythmias of right ventricular origin: cardiac magnetic resonance versus electroanatomic mapping. *J Cardiovasc Electrophysiol* 2011. doi: 10.1111/j.1540-8167.2011.02127.
37. Fabritz L, Hoogendijk MG, Scicluna BP, van Amersfoorth SC, Fortmueller L, Wolf S, Laakmann S, Kreienkamp N, Piccini I, Breithardt G, Noppinger PR, Witt H, Ebnet K, Wichter T, Levkau B, Franke WW, Pieperhoff S, de Bakker JM, Coronel R, Kirchhof P. Load-reducing therapy prevents development of arrhythmogenic right ventricular cardiomyopathy in plakoglobin-deficient mice. *J Am Coll Cardiol* 2011;**57**:740–750.